

See discussions, stats, and author profiles for this publication at: <https://www.researchgate.net/publication/233790656>

# Spontaneous and electric field induced quadratic optical nonlinearity in ferroelectric crystals $\text{AgNa}(\text{NO}_2)_2$

ARTICLE *in* APPLIED PHYSICS LETTERS · FEBRUARY 2010

Impact Factor: 3.3 · DOI: 10.1063/1.3315941

CITATIONS

4

READS

41

5 AUTHORS, INCLUDING:



**Andriy V. Kityk**

Czestochowa University of Technology

206 PUBLICATIONS 1,935 CITATIONS

SEE PROFILE



**Robert Czaplicki**

Tampere University of Technology

48 PUBLICATIONS 253 CITATIONS

SEE PROFILE



**A. S. Andrushchak**

Lviv Polytechnic

63 PUBLICATIONS 291 CITATIONS

SEE PROFILE



**Bouchta Sahraoui**

University of Angers

384 PUBLICATIONS 2,978 CITATIONS

SEE PROFILE

# Spontaneous and electric field induced quadratic optical nonlinearity in ferroelectric crystals $\text{AgNa}(\text{NO}_2)_2$

A. V. Kityk,<sup>1,a)</sup> R. Czaplicki,<sup>2</sup> A. Klöpperpieper,<sup>3</sup> A. S. Andrushchak,<sup>4</sup> and B. Sahraoui<sup>2</sup>

<sup>1</sup>Faculty of Electrical Engineering, Czestochowa University of Technology, Al. Armii Krajowej 17, 42-200 Czestochowa, Poland

<sup>2</sup>Laboratoire POMA, FRE CNRS 2988, Université d'Angers, 2 Boulevard Lavoisier, 49045 Angers Cedex, France

<sup>3</sup>Technische Physik, Universität des Saarlandes, 66041 Saarbrücken, Germany

<sup>4</sup>Lviv Polytechnic National University, 12 S. Bandera Str., 79013 Lviv, Ukraine

(Received 30 November 2009; accepted 21 January 2010; published online 11 February 2010)

We demonstrate the second harmonic generation (SHG) in ferroelectric  $\text{AgNa}(\text{NO}_2)_2$  crystals resulting from the spontaneous and electric field induced polarizations. Relatively high effective nonlinear optic (NLO) susceptibility is combined in this crystals with the existing several phase matching geometries of NLO interaction. Anomalously large response of SHG with respect to an applied electric field has been found in the vicinity of the paraelectric-to-ferroelectric phase transition. The behavior of NLO properties in the ferroelectric phase and especially in the region of the Curie point is discussed within the phenomenological theory. © 2010 American Institute of Physics. [doi:10.1063/1.3315941]

Ferroelectric materials are considered as very promising materials for a number of applications being usually related to their large nonlinear response with respect to the electromagnetic radiation in the optical range. Corresponding effects include electro-optic, second harmonic generation (SHG), parametric amplification and generation, or other nonlinear optic (NLO) or parametrical optic phenomena widely used for the light modulation or its frequency conversion.<sup>1,2</sup>

In this letter we demonstrate the quadratic optical nonlinearity resulting from spontaneous and electric field induced polarizations in silver sodium nitride [ $\text{AgNa}(\text{NO}_2)_2$ , hereafter SSN] crystals. To probe such nonlinearity the SHG, being represented as  $\chi^{(2)}$ -nonlinear frequency-conversion processes, has been chosen as the most appropriate technique. SSN crystals exhibit the phase transition (PT) at  $T_c \approx 38^\circ\text{C}$  (Refs. 3 and 4) from a paraelectric phase (space group  $D_{2h}^{24}$ ) to the proper ferroelectric phase (space group  $C_{2v}^{19}$ ). Comprehensive dielectric,<sup>3-5</sup> specific-heat,<sup>6</sup> and elastic measurements have revealed that the PT is of first order, but very close to second order one. Ferroelectricity in SSN appears due to an ordering of the  $\text{NO}_2^-$  dipoles which at room temperature give quite large spontaneous polarization (about  $8 \mu\text{C}/\text{cm}^2$ ) being oriented along  $[010]$  crystallographic direction.<sup>4</sup>

Single SSN crystals were grown from aqueous solution containing 9.8 wt %  $\text{AgNO}_2$  and 37.2 wt %  $\text{NaNO}_2$  by the slow evaporation method at constant temperature ( $\sim 25^\circ\text{C}$ ). We used the standard crystallographic orientation for the paraelectric phase:  $a=8.05 \text{ \AA}$ ,  $b=10.77 \text{ \AA}$ , and  $c=10.76 \text{ \AA}$ . Crystals SSN are yellowish with the perfect cleavage plane parallel to  $[101]$ - and  $[10\bar{1}]$ -directions. Accordingly, the geometry of samples was adjusted to these planes, i.e., we used the slabs or plates having perfectly cleaved faces  $[101]$  (or  $[10\bar{1}]$ ) without further polishing and

with deposited silver paste electrodes on conventionally polished  $[010]$ -faces. The SHG has been excited by means of nanosecond IR Q-switched laser Vector 1064–3000–30 ( $\lambda = 1064 \text{ nm}$ ) and registered in a standard setup described earlier in Ref. 8. The sample has been set into thermostabilized optical cell and rotated by means of a step motor with angular step of  $0.01^\circ\text{C}$  and rotation speed  $1\text{--}5^\circ\text{C}/\text{min}$ . The accuracy of the temperature stabilization was about  $0.01^\circ\text{C}$ .

In the ferroelectric phase SSN crystals exhibit only a very weak intensity SHG if the incident light propagates exactly along the  $[101]$ -direction which may be explained by a lack of phase matching between the interacting waves in this direction. Nevertheless, the phase matching indeed can be achieved in slightly tilted geometry. The inset (a) in Fig. 1 demonstrate the example of such phase matching geometry (PMG) defined by the tilt angle  $\theta_p$  and azimuthal angle  $\varphi_p$ . Here the incident laser beam ( $\lambda = 1064 \text{ nm}$ ) is polarized vertically and outgoing intense SHG ( $\lambda = 532 \text{ nm}$ ) exhibits nearly horizontal polarization at small  $\theta_p$ . One should be emphasized, that the measurements have been performed on

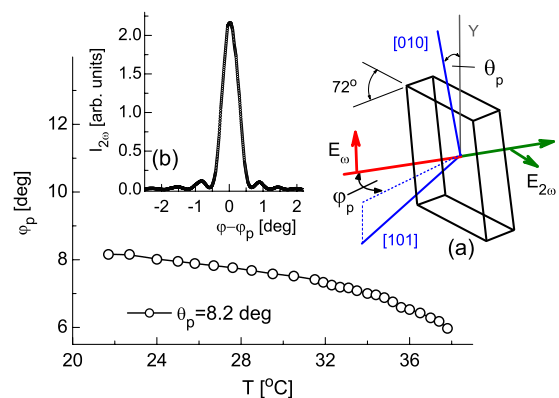


FIG. 1. (Color online) Temperature dependence of the phase matching angle  $\varphi_p$  being measured at the fixed tilt angle  $\theta_p=8.2^\circ$ . Inset (a): phase matching geometry in SSN crystals. Inset (b): Maker fringe pattern in the vicinity of the phase matching angle  $\varphi_p$  (thickness  $d=0.6 \text{ mm}$ ).

<sup>a)</sup>Electronic mail: andriy.kityk@univie.ac.at.

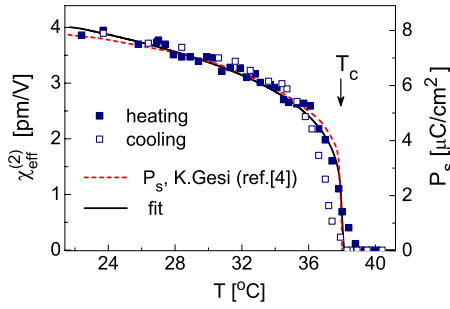


FIG. 2. (Color online) Temperature dependences of  $\chi_{\text{eff}}^{(2)}$  determined at heating and cooling in PMG. Red dashed line marks the temperature behavior of the spontaneous polarization  $P_s$  measured at heating in Ref. 4. Black solid line is the fit of  $\chi_{\text{eff}}^{(2)}(T)$ -dependence measured at heating.

fresh samples being cut from the crystals that were grown in the ferroelectric phase. Obtained in such a way crystals are usually single domain and for this reason we believe that we deal with the birefringent phase matching rather than with so-called quasiphasematching provided by a regular ferroelectric domain structure. The  $\varphi$ -dependence of SHG intensity  $I_{2\omega}$  reveals Maker-fringe pattern [Fig. 1, inset (b)]. At the fixed tilt angle  $\theta = \theta_p$  the other phase matching angle  $\varphi_p$  is only weakly temperature dependent in the ferroelectric phase (see Fig. 1). Thus the variation of the effective second order NLO susceptibility  $\chi_{\text{eff}}^{(2)}(T)$  scales with the temperature dependence of  $I_{2\omega}^{1/2}$  measured at PMG. Comparing it with the intensity of SHG in  $\text{SiO}_2$  ( $\chi_{111}$ -component) one obtains at  $T = 23^\circ\text{C}$  the magnitude  $\chi_{\text{eff}}^{(2)} = 4.0$  pm/V. Moreover, our evaluations reveal that the weight factors bonded to the partial contributions of symmetry allowed tensor components  $\chi_{ijk}^{(2)}$  into the effective NLO susceptibility  $\chi_{\text{eff}}^{(2)}$  either do not depend at all or change only slightly with temperature due to a weakly varying  $\varphi_p(T)$ -dependence. Corresponding corrections appear thus beyond the accuracy of our measurements and will be ignored in further analysis.

Figure 2 shows the temperature dependences of  $\chi_{\text{eff}}^{(2)}$  measured in PMG at heating and cooling. As one expects, the PT from the ferroelectric to paraelectric phase is characterized by vanishing of SHG, however variation of  $\chi_{\text{eff}}^{(2)}(T)$  in the vicinity of Curie point appears to be gradual with a lack of a jump characteristic for the first order PTs. Both at heating and cooling the PT appears to be smeared in the temperature interval of about  $1.5^\circ\text{C}$  and is characterized by the temperature hysteresis of about  $0.5^\circ\text{C}$ . In the ferroelectric phase  $\chi_{\text{eff}}^{(2)}(T)$  well scales with the temperature dependence of spontaneous polarization  $P_s(T)$  measured in Ref. 4 (see red dashed line in Fig. 2). We interpret such behavior within the phenomenological Landau theory of second order PTs. In the case of  $\text{D}_{2h}^{24} \rightarrow \text{C}_{2v}^{19}$  transition the free energy takes the form

$$F = F_P + F_{\text{int}},$$

$$F_P = \frac{1}{2}A(T - T_0)P^2 + \frac{1}{4}BP^4 + \frac{1}{6}CP^6 - PE,$$

$$F_{\text{int}} = -\alpha_{ijmn}^{0,k,k,2k}[P_i(0)P_j(k)P_m(k)P_n(-2k) + c \cdot c] + \frac{1}{2\kappa_{ii}^{(K)}}P_i(K)P_i(-K), \quad (1)$$

where  $F_P$  is the free energy expansion on the  $Y$ -component

of the polarization  $P$  being the order parameter of this model,  $A$ ,  $B$ , and  $C$  are the free energy expansion coefficients,  $T_0$  is the Curie–Weiss temperature,  $\alpha_{ijmn}^{0,k,k,2k}$  are the coupling constants,  $\kappa_{ii}^{(K)} = \epsilon_0 \chi_{ii}(K)$ ,  $\epsilon_0$  is the vacuum permittivity and  $\chi_{ii}(K)$  are the components of the inhomogeneous linear dielectric susceptibility at the wavevector  $K$ .  $F_{\text{int}}$  includes  $\alpha$ -terms representing the invariants with respect to the rotational-translational operations of  $\text{D}_{2h}^{24}$  space group and indeed describe the interaction between the static homogeneous polarization  $P_i(0)$ , inhomogeneous polarizations  $P_j(k)$  and  $P_m(k)$ , being induced by the light, and its second harmonic  $P_n(2k)$ . In the simplest approximation one ignores the static polarization resulting from the NLO conversion. Then at  $E=0$  the minimization of  $F$  with respect to  $P$  and  $P_n(2k)$  yields  $|P_n(2k)| = 2\alpha_{2jmn}^{(0,k,k,2k)}\kappa_{nn}^{(2k)}P_s|P_j(k)||P_m(k)|$  where  $P_s$  is the equilibrium value of spontaneous polarization being equal to 0 above the Curie point  $T_c = T_0 + 3B^2/16AC$  and defined as  $P_s^2 = (-B + \sqrt{B^2 - 4CA(T - T_0)})/2C$  at  $T < T_c$ . Accordingly,  $\chi_{njm}^{(2)} \propto \alpha_{2jmn}^{(0,k,k,2k)}\kappa_{nn}^{(2k)}P_s$  thus NLO susceptibility may be viewed as such which is resulted from the spontaneous polarization, i.e., one may call it as *spontaneous SHG* in analogy to the terminology used for the characterization of electro-optical properties in ferroelectrics (see e.g., Ref. 9). More general form of this equation ignores an origin of the polarization itself, i.e.,  $\chi_{njm}^{(2)} \propto \alpha_{2jmn}^{(0,k,k,2k)}\kappa_{nn}^{(2k)}P$ . Here  $P$  implies the total polarization being presented as superposition of  $P_s$  and  $P_{\text{ind}}$ , where  $P_{\text{ind}} = \epsilon_0(\epsilon_{22} - 1)E \approx \epsilon_0\epsilon_{22}E$  is the induced polarization caused by an applied external field ( $\vec{E} \parallel \mathbf{Y}$ ) and  $\epsilon_{22}$  is the dielectric constant. In the paraelectric phase and at  $E=0$  the SHG is not observed since  $P_s=0$  and all the tensor components  $\chi_{njm}^{(2)}=0$ . However, the SHG may be induced here by applying an external electric field along the ferroelectric axis. In this case  $\chi_{njm}^{(2)} \propto \alpha_{2jmn}^{(0,k,k,2k)}\kappa_{nn}^{(2k)}\epsilon_0\epsilon_{22}E$  thereby one expects its anomalous increase in the vicinity of the Curie point  $T_c$  keeping in mind that the dielectric constant  $\epsilon_{22}$  of proper ferroelectric SSN is subjected to the Curie–Weiss law:  $\epsilon_{22}(T) \propto C_0(T - T_0)^{-1}$ ,  $C_0$  is the Curie–Weiss constant.<sup>3</sup> An independent symmetry interpretation of this phenomena may be given basing on the Curie principle. Following to it the electric field applied along the  $Y$ -axis lowers the crystal symmetry from the centrosymmetric point group  $mmm$  to a non-centrosymmetric (polar) group  $mm2_y$  thus the SHG becomes to be symmetry allowed if  $E \neq 0$ .

Figure 3 demonstrates the SHG in the centrosymmetric paraelectric phase of SSN crystals induced by applied electric field  $\vec{E} \parallel \mathbf{Y}$ . Far above  $T_c$  the field dependences  $\chi_{\text{eff}}^{(2)}(E)$  are nearly linear, however closer to  $T_c$  they become more non-linear and finally even get a saturated character. The constant  $\beta$ , defined as derivative  $d\chi_{\text{eff}}^{(2)}/dE \propto dP_{\text{ind}}/dE \propto \epsilon_{22}$ , represents the third order nonlinear susceptibility. Figure 4 shows the constant  $\beta$ , being determined at  $E \rightarrow 0$ , and its inverse magnitude  $\beta^{-1}$  versus  $T$ . One can realize that  $\beta(T)$  behaves in analogical manner as static dielectric constant  $\epsilon_{22}(T)$ . By extrapolating linear dependence  $\beta^{-1}(T)$  into the region below  $T_c$  one determines the temperature  $T_0$ . The difference  $\Delta T = T_c - T_0$  is only  $0.25^\circ\text{C}$  what can be considered as an evidence that we indeed deal with the PT of the first order being very close to the tricritical point.<sup>6</sup>

The anomalous behavior of  $\chi_{\text{eff}}^{(2)}(T, E \neq 0)$  near  $T_c$  (see Fig. 3) may be evaluated within the phenomenological theory by a solving the electric equation of state  $\partial F_P / \partial P$

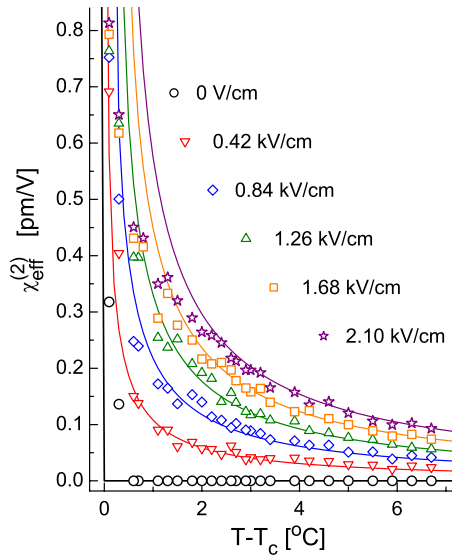


FIG. 3. (Color online) Field induced SHG in the paraelectric phase. Points correspond to  $\chi_{\text{eff}}^{(2)}$  vs  $T$  measured in PMG at different magnitudes of the external electric field  $E$  being applied along the  $Y$ -axis. Solid lines are the best fits obtained by solving the electric equation of state.

$=A(T-T_0)P+BP^3+CP^5-E=0$  for each particular temperature  $T$ . Solid colored lines in Fig. 3 and black line in Fig. 2 are the best fits that have been obtained applying the set of the free energy parameters (in SI units):  $A=1.6 \times 10^7$ ,  $B=-1.0 \times 10^9$ , and  $C=6.0 \times 10^{12}$ . One can realize that such model quite properly describes the  $\chi_{\text{eff}}^{(2)}(T, E \neq 0)$ -dependences at  $T > T_c + 1.5$  °C but evidently

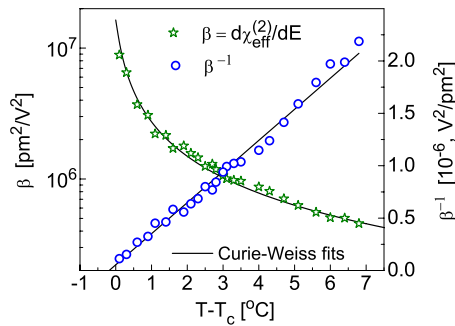


FIG. 4. (Color online) Constant  $\beta$  and its inverse magnitude  $\beta^{-1}$  vs  $T$  in the paraelectric phase. Solid black lines marks the Curie-Weiss behavior.

fails in close vicinity of  $T_c$ , especially at high applied voltages. The measured values of  $\chi_{\text{eff}}^{(2)}$  are considerably smaller here comparing to the ones expected from the theory. Such discrepancy may have a number of reasons. The most serious and very likely one may be a coexistence of metastable polar and nonpolar regions in the PT vicinity. A smeared character of the paraelectric-to-ferroelectric PT is an evidence for such coexistence indicating on a sufficiently spatially inhomogeneous structure that occurs in the region of the Curie point.

In conclusion, we have presented here the spontaneous and electric field induced SHG in SSN. In ferroelectric phase such crystal are characterized by the effective NLO susceptibilities  $\chi_{\text{eff}}^{(2)}$  being comparable or larger comparing to a number of other known NLO inorganic or organic materials (see e.g., Ref. 10). Relatively high effective NLO susceptibilities are combined in these materials with existing PMG what makes them rather perspective for a number of NLO applications such as e.g., SHG, parametric NLO generation or amplification or other applications that deal with the frequency conversion. In addition, an anomalously large response of NLO properties with respect to applied electric field has been found in the vicinity of the Curie point. This may also have a number of applications, especially there, where a high-efficient control and/or tuning of the SHG intensity are required.

This work has been supported by grant Moltech-Anjou (Angers, France).

<sup>1</sup>B. E. A. Saleh and M. C. Teich, *Fundamentals of Photonics* (Wiley, New York, 1991).

<sup>2</sup>F. Agulló-López, J. M. Cabrera, and F. Agulló-Rueda, *Electro-Optics, Phenomena, Materials, and Applications* (Academic, New York, 1994).

<sup>3</sup>K. Gesi, *J. Phys. Soc. Jpn.* **28**, 395 (1970).

<sup>4</sup>K. Gesi, *J. Phys. Soc. Jpn.* **33**, 108 (1972).

<sup>5</sup>J. Petersson, E. Schneider, and R. Siems, *Z. Phys. B: Condens. Matter* **39**, 233 (1980).

<sup>6</sup>J. Helwig, J. Petersson, and E. Schneider, *Z. Phys. B* **28**, 87 (1977).

<sup>7</sup>V. P. Soprunyuk, A. Fuith, H. Kabelka, K. Knorr, A. Klöpperpieper, K. Sokalski, and A. V. Kityk, *Phys. Rev. B* **66**, 104102 (2002).

<sup>8</sup>B. Sahraoui, J. Luc, A. Meghea, R. Czaplicki, J.-L. Fillaut, and A. Migalska-Zalas, *J. Opt. Pure Appl. Opt.* **11**, 024005 (2009).

<sup>9</sup>L. G. Lomova, A. S. Sonin, and T. A. Regulskaya, *Sov. Phys. Crystallogr.* **13**, 68 (1968).

<sup>10</sup>A. Keens and H. Happ, *J. Phys. C* **21**, 1661 (1988); W. Bi, N. Louvain, N. Mercier, J. Luc, I. Rau, F. Kajzar, and B. Sahraoui, *Adv. Mater.* **20**, 1013 (2008).